Fluorescence hole-burning and site-selective studies of LHCII

Gibasiewicz, K.; Rutkowski, M.; van Grondelle, R.

published in
Photosynthetica
2009

DOI (link to publisher)
10.1007/s11099-009-0037-0

document version
Publisher's PDF, also known as Version of record

Fluorescence hole-burning and site-selective studies of LHCII

K. GIBASIEWICZ[*,+], M. RUTKOWSKI[*], and R. VAN GRONDELLE[**]

Department of Physics, Adam Mickiewicz University, ul. Umultowska 85, 61-614 Poznań, Poland[*]
Department of Physics and Astronomy, Vrije Universiteit, De Boelelaan 1081,1081 HV Amsterdam, The Netherlands[**]

Abstract

We report the observation of two types of changes in fluorescence spectra of LHCII at 4.2 K following intense illumination of the sample with a spectrally narrow laser beam at wavelengths between 678 and 686 nm. Nonspecific changes (burning-wavelength independent) are characterized by two relatively broad bands: a positive one at ~ 678.7 nm and a negative one at ~ 680.8 nm. These changes reveal a ~1.3-nm blue shift of the distribution of final emitters in LHCII, from 680.3 nm to ~ 679.0 nm independent of the excitation wavelength. Specific fluorescence changes (burning-wavelength dependent) are characterized by a sharp hole exactly at the burning wavelength, and positive changes directly to the shorter- and longer-wavelength side of the narrow hole. The negative changes are interpreted as zero-phonon holes, while the positive features are assigned to non-photochemical products. In the low-burning intensity experiment, in addition to the zero-phonon holes, we observed also the holes to the longer wavelength of the zero-phonon hole, which were assigned to a sum of phonon and pseudo-phonon side bands. The shapes of these extra holes are identical to the shapes of the holes revealed in the fluorescence line narrowing experiment. On the basis of the low-burning intensity experiment we estimated the upper limit of the electron-phonon coupling strength for LHCII, characterized by a Huang-Rhys factor of 1.5.

Additional key words: chlorophyll, fluorescence, light-harvesting complex II, line-narrowing, zero-phonon line.

Introduction

Photosynthesis is the process by which solar light energy is converted into the energy of chemical bonds occurring in plants, algae and photosynthetic bacteria (Blankenship 2002). The primary processes of photosynthesis include light absorption in the antenna pigment-protein complexes, excitation energy migration from antenna to another specialized pigment-protein complex called the reaction center (RC), and electron transfer reactions in RC. In oxygenic photosynthesis there are two types of RCs: Photosystem II (PSII) and Photosystem I (PSI). LHCII, or the light-harvesting complex II, is a main component of the PSII antenna system, and is involved not only in the light harvesting but also in different mechanisms regulating the distribution of excitation energy between PSII and PSI (state transitions, Allen 2003) and protecting PSII RC from the excess of light (non-photochemical quenching; Ruban *et al.* 2007). The basis for understanding the role of LHCII in all these processes is the detailed knowledge of the spectroscopic properties of this complex (van Amerongen and van Grondelle 2001) in relation to its structure (Liu *et al.* 2004).

Photosynthetic pigment-protein complexes, including light-harvesting complex II (LHCII), were successfully studied with the use of absorption hole-burning (AHB; Reinot *et al.* 2001, Ihalainen *et al.* 2003). This well-established technique is based on the measurement of the absorption spectra before and after intense illumination of the sample with a spectrally narrow light beam at low temperatures. The light usually burns deep narrow holes in the absorption spectra, coincident with the illumination or burning wavelengths. These zero-phonon holes (ZPH) are of non-photochemical or photophysical origin which means that the loss of absorption is due to a small rearrangement of the burned individual molecules. This loss is compensated by absorption increase (antiholes) towards longer and shorter wavelengths of the hole (Johnson *et al.* 1991). Very often, additional holes

Received 18 December 2008, *accepted* 9 June 2009.
[+]Corresponding author; fax: +48 61 8295155, e-mail: krzyszgi@amu.edu.pl
Acknowledgements: K.G. gratefully acknowledges financial support from Netherlands Organisation for Scientific Research (NWO; grant B 81-734) and a generous gift of LHCII preparations from C. Ilioaia.
Abbreviations: AHB – absorption hole burning, Chl – chlorophyll, EET – excitation energy transfer, FHB – fluorescence hole burning, FLN – fluorescence line narrowing, LHCII – light-harvesting complex II, PSI – photosystem I, PSII – photosystem II, PSB – phonon side band, PPSB – pseudo-phonon side band, RC – reaction center, SSF – site selective fluorescence, ZPH – zero-phonon hole, ZPL – zero-phonon line.

covering different regions of the absorption spectrum are observed. These additional holes may reveal: (*1*) coupling of the electronic transitions in the pigment molecules to the vibrations of the protein environment (called electron-phonon coupling; Gillie *et al.* 1989a, Pieper *et al.* 1999, 2001, Hayes *et al.* 2000, Ihalainen *et al.* 2003), (*2*) coupling of the electronic transitions to the vibrations in the pigment molecules (Gillie *et al.* 1989b), (*3*) existence of the excitonic coupling between different pigment molecules (Reddy *et al.* 1994), (*4*) excitation energy transfer from the higher to the low energy states (red Chls; Hayes *et al.* 2000, Rätsep *et al.* 2000, Zazubovich *et al.* 2002, Ihalainen *et al.* 2003). Furthermore, analysis of the AHB spectra gives insight into spectral characteristics of individual molecules and their distributions (homogeneous and inhomogeneous broadening) as well as into the excited state dynamics (Reddy *et al.* 1994, Groot *et al*. 1996, Pieper *et al.* 1999, Dědic *et al*. 2004).

A technique complementary to AHB, also well-established, is the fluorescence line narrowing (FLN; Peterman 1998, Pieper *et al.* 2001, Timpmann *et al.* 2004, Gibasiewicz *et al.* 2005, Rätsep *et al.* 2005). In photosynthetic complexes, low temperature emission originates from a distribution of the lowest-energy states. This emission is preceded by excitation energy transfer (EET) from the higher energy states. Selective, narrow-band excitation with increasing wavelength results in emission only from a sub-distribution of the lowest-energy states characterized by the wavelengths longer than that of the exciting light, which leads to the narrowing of the site selective fluorescence spectra. The absorption spectra of individual pigments (usually chlorophylls, Chls) at low temperatures are composed of a zero-phonon line (ZPL) corresponding to the pure 0-0 electronic transition and of a phonon wing or phonon side-band (PSB) to the shorter wavelengths of the ZPL, due to the electron-phonon coupling (the respective fluorescence spectra of the individual pigments show a PSB at the opposite longer-wavelengths side of the ZPL). Therefore, selective excitation of the final emitters (not followed by any EET to other pigments) into the long wavelength tail of absorption spectrum shows an increased probability of exciting the pigments *via* their ZPL and permits observation of the fluorescence PSB of individually excited molecules. Of course, the same light also excites a certain fraction of pigments *via* their absorption PSB and therefore, the FLN spectra contain, apart from the PSB, also a pseudo-phonon side band (PPSB). FLN spectra also reveal intramolecular vibrations coupled to 0-0 electronic transitions (Wolf *et al.* 1996, Peterman *et al.* 1997, Rätsep and Freiberg 2007, Rätsep *et al.* 2008).

LHCII, the most abundant peripheral pigment-protein antenna complex involved in plant photosynthesis, is associated with PSII and occurs in the form of trimers (Barber and Kühlbrandt 1999, Boekema *et al.* 1999, 2000). Each of the monomers forming the trimer contains 8 chlorophylls *a* (Chls *a*) and 6 Chls *b* (Liu *et al.* 2004). LHCII attracts a lot of attention because of its role in non-photochemical quenching and state transitions (Allen 2003), which are the two regulatory processes not well understood yet. Numerous results of spectroscopic studies on LHCII were reviewed by van Amerongen and van Grondelle (2001) and can also be found in Croce *et al.* (2001). On the basis of the disordered exciton model and the Redfield relaxation theory, a detailed model was proposed for the exciton level structure and energy transfer/exciton relaxation pathways in LHCII. In this model the lowest exciton level of the Chl trimer composed of Chls *a* 610, 611 and 612 (the numbers denoting particular Chls are according to the structure reported by Liu *et al.* 2004), is the main red emitter in LHCII (Novoderezhkin *et al.* 2005, van Grondelle and Novoderezhkin 2006).

AHB was used to determine the ~ 680-nm energy level and inhomogeneous width (70-120 cm^{-1}) of the lowest energy state responsible for the LHCII emission at low temperatures (Reddy *et al.* 1994, Pieper *et al.* 1999). Further, both AHB and FLN techniques were applied to investigate the electron-phonon coupling, which was concluded to be weak, and characterized by a mean phonon frequency ω_m = 15–18 cm^{-1} and Huang-Rhys factor, S = 0.8–0.9 (Pieper *et al.* 1999, 2001). On the basis of the FLN studies, the 105-cm^{-1} width of the one-phonon profile of individual emitters was found to be strongly asymmetric with a much steeper shorter than longer-wavelength slope (Pieper *et al.* 2001).

Unlike AHB and FLN, the fluorescence hole-burning (FHB) with non-selective excitation was rarely applied in the studies of photosynthetic complexes (Hala *et al*. 1992, Groot *et al*. 1996, Fetisova and Mauring 1998, Dědic *et al*. 2004). FHB is a technique complementary to both AHB and FLN. Similarly to AHB it allows measurements of ZPH, PSB and PPSB, and estimation of the strength of electron-phonon coupling. In this contribution we present a systematic FHB study combined with site selective fluorescence (SSF) study of LHCII. The results are compared with the earlier findings from AHB and FLN studies.

Materials and methods

Plants: LHCII trimeric complexes were prepared from dark-adapted spinach leaves by an isoelectric focusing procedure as described (Ruban *et al.* 1994). Immediately after the treatment, the samples were further purified in the seven-step exponential sucrose gradient from 0.15 to 0.87 M sucrose. The concentrated sample was diluted before the fluorescence experiments in a buffer containing 20 mM Bis Tris (pH = 6.0), 10 mM NaCl,

5 mM $CaCl_2$, 0.06% n-dodecyl-beta-D-maltoside, and 60 % (v/v) glycerol.

Methods: A diluted sample ($OD_{676nm,10mm} \approx 0.1$) was placed in a (10 mm × 10 mm plastic) cuvette and frozen to 4.2 K in a liquid helium cryostat (Utreks; Kiev, Ukraine). Both FHB and SSF experiments were performed with the setup described previously (Gibasiewicz *et al.* 2005). Shortly, the source of the nonselective excitation at 420 nm in the FHB experiment was a 150-W tungsten halogen lamp equipped with an interference filter (fwhm = 20 nm). The hole-burning light of ~ 0.1-1 W m^{-2} power density and of tunable wavelength was supplied by a dye laser (*CR 599, Coherent*; Santa Clara, USA) pumped by an argon ion laser (*Innova 310, Coherent*; Santa Clara, USA). In SSF experiment the same dye laser, but of attenuated power density, was used as a source of the wavelength-selective excitation. The nonselective and selective light beams entered the sample from two opposite sides of the sample cuvette and the fluorescence light was collected at 90 degrees to the direction of the excitation beams. The fluorescence emission spectra were measured with a cooled CCD camera (*Chromex ChromCam, Bruker Optics*; Ettlingen, Germany) equipped with a 0.5-m spectrograph (*Chromex 500IS, Bruker Optics*; Ettlingen, Germany). The measured spectral width of the very narrow dye laser lines was 0.4 nm whereas the measurements of the spectral bands' position were one order of magnitude more accurate. To obtain the spectra at the near detector-saturating limit and, thus, of high signal to noise ratio, we accumulated, in experiments with non-selective excitation at 420 nm, the fluorescence signal for a typical time of 0.1 s. In the SSF experiment, the accumulation time was gradually increased from 1 s to a few seconds with increasing wavelengths of excitation. Since the peak amplitude of the scattered light (in the SSF experiment) was much higher than that of the fluorescence band, the saturation limit of the detector was exceeded around the excitation wavelength and the profile of the scattered light was slightly artificially broadened (the more the longer the accumulation time).

Nonselective fluorescence spectra were recorded before and after burning. The burning time was gradually increased from 1 to ~ 2000 s yielding a series of typically ten FHB spectra characterized by gradually increasing changes in fluorescence. The fluorescence changes were observed already after 1–2 s of burning and were still not saturated after ~ 2000 s. The burning (and selective excitation in the SSF experiment) wavelengths were tuned to eight different values: 677.6, 678.8, 679.9, 681.0, 681.8, 682.9, 683.9, and 686.3 nm. In the following, these burning/selective-excitation wavelengths are labelled by their approximate values of 678, 679, 680, 681, 682, 683, 684, and 686 nm, respectively. The majority of the FHB data presented in this paper come from the experiments with the longest burning times and correspond to a burning fluence of about 7×10^4 J m^{-2}.

For all burning wavelengths the sequence of measurements was the following: (*1*) nonselective spectrum, (*2*) selective spectrum, (*3*) illumination of the sample with the burning light (of the same wavelength as that used for the selective spectrum measurement), (*4*) selective spectrum, (*5*) nonselective spectrum, (*6*) illumination of the sample with the burning light for a longer time, again measurements of nonselective and selective spectra and so on until the total of ~ 2000 s burning time was reached. For each burning/selective-excitation wavelength a fresh sample was used.

Results

Fig. 1*A* shows the 4.2-K emission spectrum of LHCII following nonselective excitation at 420 nm. The maximum of the fluorescence band is at 680.3 nm and is by about 4 nm red-shifted relative to the maximum of the absorption spectrum (not shown). The wavelengths used for burning and selective excitation are indicated by arrows.

Three high-fluence FHB spectra are shown in Fig. 1*B*. A clear narrow hole, coincident with the burning wavelength, is observed only for burning at 681 nm. No narrow hole is observed in the 686-nm spectrum and only a very weak narrow hole is observed in the 678-nm spectrum (better seen in the 678-nm difference spectrum in Fig. 1*C*). Unlike the narrow fluorescence changes which are burning-wavelength-specific, the broad fluorescence changes are similar for all three FHB spectra: after burning, the fluorescence increases on the short-wavelength side and decreases on the long-wavelength side of the main band.

The fluorescence changes caused by burning at eight different wavelengths are compared in Fig. 1*C*. In all cases, except for the 686-nm spectrum, a narrow hole, identified as a zero-phonon hole (ZPH), is present exactly at the burning wavelength. ZPHs are accompanied by two narrow antiholes directly to the blue and to the red of the hole (nonphotochemical photoproducts, Johnson *et al*. 1991). The size of the holes and antiholes is burning-wavelength-dependent: they are the largest at 681 nm and gradually decrease towards the shorter and longer wavelengths. Clearly, in all cases, the narrow holes and antiholes are superimposed on the broad burning-wavelength-independent fluorescence changes. In line with fluorescence changes shown in Fig. 1*B*, in all cases there is a broad hole peaking at ~680.8 nm and an almost equally broad antihole at ~ 678.7 nm. These non-specific fluorescence changes are best seen in the trace 686 since they are not disturbed by any sharp, burning-wavelength-dependent features.

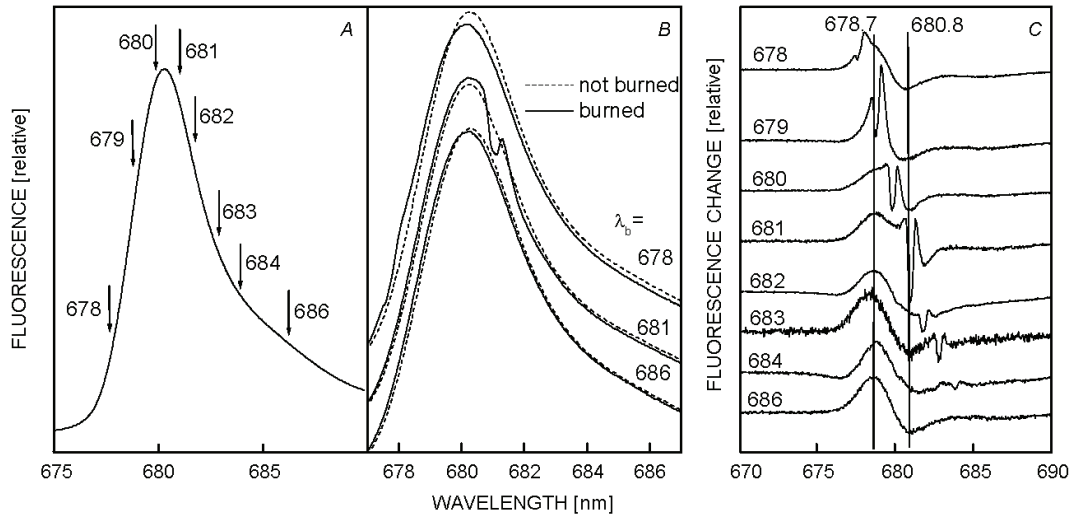

Fig. 1. Nonselective fluorescence spectra of LHCII at 4.2 K. *A*: Fluorescence spectrum with arrows indicating approximate values of burning wavelengths (*see* Material and methods for exact values). *B*: A set of three selected fluorescence spectra after hole burning at indicated wavelengths. In each case the spectrum before burning is shown for comparison. *C*: A full set of eight fluorescence difference spectra (burned minus not burned) burned at indicated wavelengths. The labelled vertical lines indicate the maxima of positive and negative bands of non-specific fluorescence changes. The burning fluence for all FHB spectra in panels *B* and *C* was ~ 7×10^4 J m^{-2}. Excitation wavelength was 420 nm for all panels.

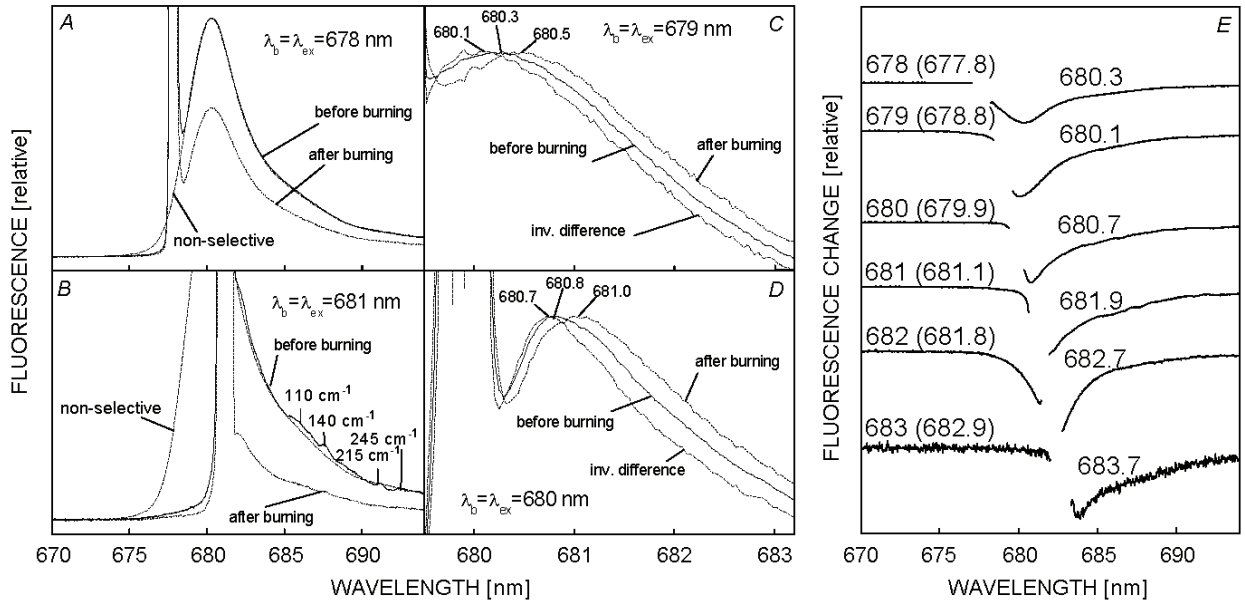

Fig. 2. Site selective fluorescence spectra of LHCII at 4.2 K recorded after selective excitation and burning at indicated wavelengths. *A,B*: Steady state site selective fluorescence spectra recorded before and after burning at 678 nm (fluence 7×10^4 J m^{-2}; *A*) and at 681 nm (fluence 7×10^4 J m^{-2}; *B*). The high-intensity peak is due to the scattered exciting light. For comparison of the shapes, the non-selective fluorescence spectra are superimposed on the long-wavelength parts of the selective spectra. Positions of vibronic bands are marked and labelled in panel *B*. *C,D*: Site selective fluorescence spectra before and after burning at two labelled burning/excitation wavelengths and the inverted difference between these two spectra. All of the three spectra are normalized to the same peak amplitude. The maxima of the fluorescence bands are labelled. *E*: Site selective fluorescence difference spectra obtained by subtracting the selective spectra recorded before burning from those recorded after burning (like those shown in panels *A* and *B*). The breaks in the continuity of the spectra are due to removing very noisy regions resulting from subtracting the scattered light peaks. For each trace, approximate excitation/burning wavelength and position of the hole minimum are given.

Fig. 2 shows the results of SSF experiments. Panel *A* shows the SSF spectra recorded after excitation at 678 nm before and after burning (at 678 nm, ~ 7×10^4 J m^{-2}). The shape of the red part of the SSF spectrum before burning is almost identical to that of the nonselective fluorescence spectrum. Also after burning, the maximum of the SSF spectrum is unaffected, although minor changes in the shape of both wings were observed (up to 0.1-nm red-shift). In contrast to the minor effect of burning on the shape of the SSF spectrum, the amplitude (and total fluorescence intensity) dropped significantly, to ~ 60% of the pre-burn amplitude, as a result of burning. Both these observations taken together indicate that: (*1*) ~ 40% of the final emitters coupled to the Chls absorbing at 678 nm were burned, (*2*) the spectral distribution of the burned emitters is not significantly different from that of all emitters, and in consequence (*3*) the excitation at 678 nm is largely followed by EET to final emitters. The last finding is indeed confirmed by the observation of a low anisotropy of the LHCII emission at 678-nm excitation (Peterman *et al.* 1997).

With increasing excitation/burning wavelengths, the shapes and/or positions of the SSF bands are modified. At 679-nm excitation, the maximum of the non-burned SSF spectrum is still at 680.3 nm but after burning (~ 7×10^4 J m^{-2}) the whole SSF band shifts about 0.2 nm to the red. Both these SSF spectra, as well as their inverted difference, normalized to the same peak amplitude, are shown in Fig. 2*C*. The inverted difference spectrum should be regarded as the spectrum of the burned chlorophylls before burning. Apparently, the emission spectrum of the Chls burned by the 679-nm beam (and also 680-nm beam; *see* below) is a bit blue-shifted relative to that of the Chls emitting after selective excitation at 679-nm (680-nm) excitation. Most likely, excitation at 679 nm (680 nm) preferentially burns directly excited final emitters, rather than secondary excitation acceptors. Coexistence of both these types of excitation energy carriers around the 680-nm excitation is indeed indicated by the intermediate anisotropy of the emission spectrum (Peterman *et al.* 1997). A similar set of spectra is shown in Fig. 2*D* for the excitation at 680 nm. Here, the spectra are much narrower than at the shorter excitation wavelengths, like in the classical fluorescence line narrowing (FLN) experiment (Pieper *et al.* 2001, Peterman *et al.* 1997). The maximum of the SSF spectrum before burning, at 680.8 nm, is 0.5-nm red-shifted relative to that obtained at the shorter excitation wavelengths and that of non-selective spectra, and undergoes even a further red-shift, to 681.0 nm, after burning (~ 7×10^4 J m^{-2}). The red slope of the SSF band is on average ~0.3 nm red-shifted as a result of burning. Burn fluence of ~ 7×10^4 J m^{-2} causes a ~ 55–70% decrease in the amplitudes of the SSF spectra for all excitation/burning wavelengths from 679 to 683 nm.

All the maxima of the SSF spectra, before and after burning, for the excitation wavelengths >680 nm are 0.8±0.1 nm (16±2 cm^{-1}) red-shifted relative to the excitation/burning wavelengths (as an example *see* the burned spectrum in Fig. 2*B*). Consequently, the minima of the SSF holes are red-shifted relative to the excitation/burning wavelengths by the same distance (Fig. 2*E*). This regular shift indicates that the bulk of the emission originates from the directly excited (*via* ZPL) lowest energy states (final emitters) and that the homogeneous broadening of the emitters is small relative to their inhomogeneous broadening (Gobets *et al.* 1994). Direct excitation of the lowest energy states is further confirmed by the appearance of vibronic structure following the excitation at 681 nm (Fig. 2*B*) (also at 680 and 682 nm). The positions of the vibronic bands at 110, 140, 215 and 245 cm^{-1} towards the red from the excitation wavelengths is in a very good agreement with the previous study of LHCII (Peterman *et al.* 1997).

Fig. 2*E* shows a set of six SSF difference spectra divided by the peak amplitudes of the respective SSF spectra before burning. As mentioned above, the minima of the traces shift towards longer wavelengths with increasing excitation wavelengths (except for the trace at 679-nm excitation which peaks at 680.1 nm). The traces 681 and 682 do not show clear minima due to very broad scattered light spectra which were cut off, whereas the trace 683 shows again a clear minimum at 683.7 nm, exactly 0.8 nm (16 cm^{-1}) towards the red from the excitation wavelength (682.9 nm). To reveal this minimum we reduced the integration time of the site selective fluorescence spectrum that resulted in the narrower spectral width of the scattered light (*see*

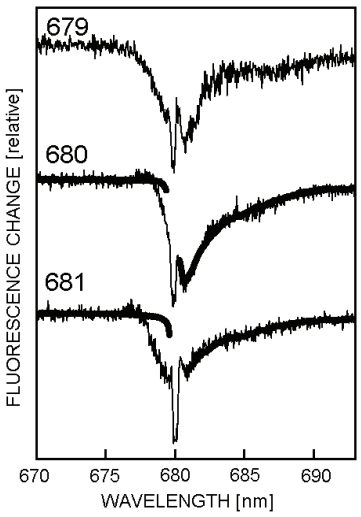

Fig. 3. Fluorescence difference spectra (burned minus not burned) burned at indicated wavelengths with light beams of low fluence (700 J m^{-2} for 679 and 200 J m^{-2} for 680 and 681). Superimposed on traces 680 and 681 are respective holes redrawn from Fig. 2*E*. The traces 679 and 681 are shifted horizontally in such a way that ZPH for all three spectra peak at ~ 680 nm.

Materials and methods) but also lowered the signal to noise ratio.

Fig. 3 shows three traces with holes burned in the fluorescence spectra in the low burning limit of 200-700 J m^{-2}. Under these conditions, neither significant specific photoproducts nor non-specific fluorescence changes were observed. Instead, apart from ZPH, a significant broader hole to the red of the ZPH was observed and interpreted as a sum of phonon- and pseudo-phonon side bands (PSB and PPSB). On the basis of the relative areas above the ZPH (A_{ZPH}) and PSB/PPSB ($A_{PSB/PPSB}$; PSB/PPSB is a sum of the PSB and PPSB contributions to the band and $A_{PSB/PPSB}$ is the area of this band), the upper limits of Huang-Rhys factor values, S, were estimated from the relation $S = \ln[(A_{PSB/PPSB}+A_{ZPH})/A_{ZPH}]$ (Jankowiak *et al.* 1993). The real values of S are lower, since they should be estimated from the relation containing the area over the pure PSB (A_{PSB}) and not a mixture of PSB and PPSB ($A_{PSB/PPSB}$). Direct access to A_{PSB}, however, is possible only applying the low temperature AHB technique, in which the PSB and PPSB are on the opposite sides of ZPH, but not in the FHB experiment. The estimated S values are 2.0 for λ_B = 679 and 680 nm, and 1.5 for λ_B = 681 nm. The higher value of S for the shorter burning wavelengths may originate from the more efficient build-up of negative non-specific fluorescence changes (*see* above). If one assumes the same contributions of PSB and PPSB in $A_{PSB/PPSB}$ at λ_B = 681 nm, and neglects the contribution from PPSB in the above formula for S, then S drops from 1.5 to 1.0 (following this assumption S is calculated from the formula: $S = \ln[(0.5*A_{PSB/PPSB}+A_{ZPH})/A_{ZPH}]$) which is in a good agreement with the value 0.9 reported for LHCII and derived from the FLN experiment (Pieper *et al.* 2001). The S value of 1.0 was also estimated on the basis of pioneering FHB experiment on LHCII (Hala *et al.* 1992). As expected, the shapes of the PSB/PPSB are, for the longer burning wavelengths and within the experimental error, identical to the shapes of the holes observed in the SSF experiment (Figs. 2*E*, 3). In particular, both experiments show that the maximum of the PSB/PPSB is 0.8-nm (16 cm^{-1}) red-shifted relative to the ZPH, which is less than the value 24 cm^{-1} reported by Pieper *et al.* (2001) in their FLN studies.

Discussion

Comparison of the excitation-selective (SSF) and non-selective (FHB) fluorescence holes: The effect of burning is much more pronounced after selective excitation in the SSF experiment than in the experiments with non-selective excitation (compare Fig. 1*B* and 2*A–B*, *E*): the holes observed in SSF are 40–70 % deep, whereas the amplitudes of the non-specific holes in FHB for all burning wavelengths are below 2 % (relative to the fluorescence peak amplitudes). This difference is easy to understand since in the SSF spectra, unlike in the FHB spectra, one expects the emission only from the same population of Chls which is largely burned away. No non-specific photoproducts of burning are observed in the SSF spectra, due to the selective excitation (photo-products absorb at different wavelengths). For the same reason, the SSF spectra also do not contain the specific photoproducts, and specific ZPH are hidden by the intense scattered excitation light. Additionally, emission at 678-nm excitation is preceded by EET (*see* Results) like in non-selective FHB spectra. In effect, the SSF holes at short-wavelength excitation (678 nm, Fig. 2*E*) are similar to the non-specific holes observed in FHB difference spectra (Fig. 1*C*).

The changes in the shape and position of the SSF bands with increasing burning/excitation wavelength before and after burning (Fig. 2*C–D*), imply that the SSF holes, unlike FHB non-specific holes, shift and change their shapes as a function of the burning/excitation wavelengths (Fig. 2*E*). This apparent discrepancy is caused by the fact that the longer-wavelength selective excitations may probe only fractions of energy states which are even lower than those corresponding to the excitation wavelengths. In consequence, longer-wavelength-excitation SSF holes are similar to the low-fluence specific FHB holes (Fig. 3).

Comparison of the fluorescence and absorption hole-burning spectra of LHCII: The specific and non-specific fluorescence changes in the FHB experiment (Fig. 1*C*) are strikingly similar to the results of AHB studies of LHCII (Pieper *et al*. 1999, Reddy *et al*. 1994). In these studies, narrow holes in the absorption spectra were observed at the wavelengths coincident with the burning wavelengths ranging from ~ 650 to 681 nm. Additionally, a broad hole centred at 679–680 nm, accompanied by a broad antihole at 676 nm was observed for burning wavelengths ≤670 and 677.5 nm (Fig. 3 in Reddy *et al*. 1994).

The burning efficiency of ZPH depends on the burning wavelengths in the FHB experiment (Fig. 1*C*) in a similar way as in the AHB experiment (Reddy *et al*. 1994, Pieper *et al*. 1999) except for the fact that in FHB the efficiency is maximal at 681 nm whereas in AHB at 678 nm. ZPH at the 678-nm excitation is shallow in FHB because in this technique, the size of ZPH is determined not only by the hole-burning efficiency of particular spectral forms of pigments but also by the spectral distribution of final emitters represented by the steady-state fluorescence spectrum (Fig. 1*A*) which shows a low amplitude at 678 nm.

The non-specific fluorescence changes with maxima of the hole and antihole at 680.8 and 678.7 nm, respectively (Fig. 1*C*), are narrower and red-shifted compared to the respective absorption changes at 679–680 and 676 nm

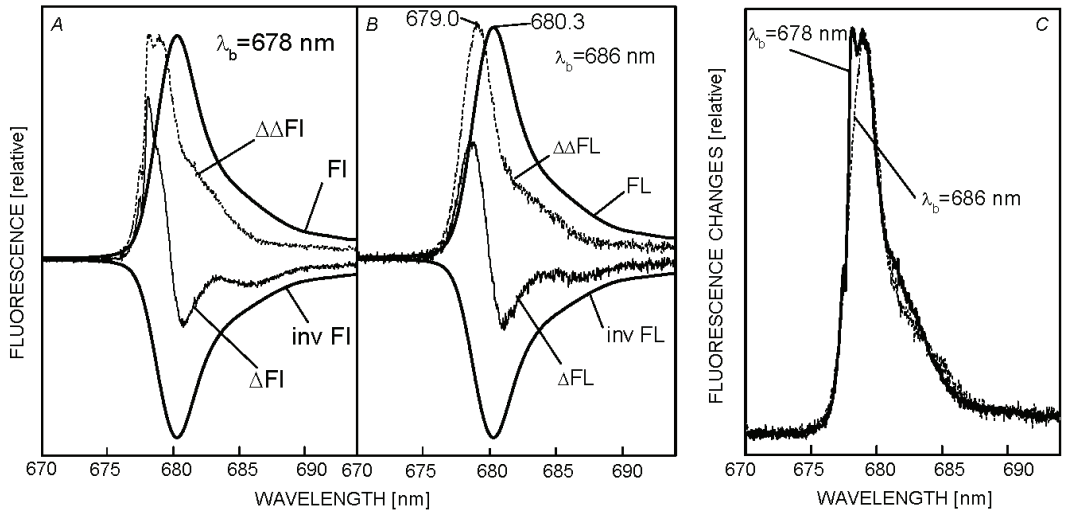

Fig. 4. Decomposition of the fluorescence difference spectra burned at 678 (*A*) and 686 nm (*B*) (redrawn from Fig. 1 *C*) onto the negative (inv Fl) and positive (ΔΔFl) components. The resulting ΔΔFl spectra peak at 679.0 nm and are ~3 nm wide (FWHM). For comparison, non-selective fluorescence spectrum, FL, is shown (*A*, *B*). It peaks at 680.3 nm and is 4.2-nm wide (FWHM). *C*: Comparison of the shapes of ΔΔFl spectra from panels *A* and *B*. *See* text for further details.

(Reddy *et al*. 1994, Pieper *et al*. 1999). The broad absorption hole at 679–680 was previously assigned to photobleaching of an inhomogeneously broadened lowest energy state in LHCII giving rise to the fluorescence origin at 680.3 nm. We agree with this assignment and in the following we present an analysis showing that the fluorescence hole peaking at 680.8 nm (and antihole peaking at 678.7 nm) originates from the blue-shift of the fluorescence origin from 680.3 to ~ 679.0 nm.

The origin of the non-specific fluorescence changes: Fig. 4*A* shows the fluorescence changes recorded after burning at 678 nm (ΔFl), the inverted non-selective fluorescence spectrum (inv Fl) and the difference between these two spectra (ΔΔFl). Thus, the differential-like shape of the non-specific fluorescence changes may be regarded as due to a ~1.3-nm blue-shift of the fluorescence origin (compare ΔΔFl and Fl). Analogous analysis has been performed for the burning at 686 nm (Fig. 4*B*). The shapes of the resulting ΔΔFl signals from panels *A* and *B* are compared in panel *C*. They are very similar to each other (the only differences are the specific changes superimposed on the non-specific changes in the 678-nm trace and minor differences in the shapes of the wings at $\lambda > 681$ nm). This similarity has a few consequences. First of all, it indicates that the non-specific burning effect is almost identical for the two so much different burning wavelengths (also for the other wavelengths, Fig. 1*C*). These identical effects for a broad range of burning wavelengths are surprising. In previous papers (Reddy *et al*. 1994, Pieper *et al*. 1999) the broad non-specific burn-induced absorption changes were suggested to originate from burning of a wide spectral distribution of long-lived lowest energy excited states which are quickly populated after ultrafast excitation energy transfer (EET) from directly excited higher-energy states. We observed the fluorescence changes in the 678.7–680.8-nm range even after burning at 682–686 nm (Fig. 1*C*) when the uphill EET should be blocked at 4.2 K. At all burning wavelengths the size of the non-specific fluorescence changes was linearly dependent on the fluence. On the basis of these observations, we suppose that the non-specific fluorescence changes reveal some general vulnerability of LHCII which undergoes some structural/interaction changes, in response to absorption of high-intensity light of any wavelength and dissipation of its energy. As a result, a change in the Chl-Chl and Chl-protein coupling may occur and a blue-shift of the red-most emission is observed. Since the red-most state in LHCII was previously proposed to be localized mainly on Chl *a* 610 (Novoderezhkin *et al*. 2005, van Grondelle and Novoderezhkin 2006) we hypothesize that the interactions of this Chl are modified by the heat-dump related structural changes in LHCII. Because of the statistical character of these modifications together with the red-shift of Chl *a* 610 in native samples, the net effect of the excessive heat dissipation is a blue-shift. The broad non-specific fluorescence changes can also be contributed to by a burning effect of the weak non-selective excitation at 420 nm.

References

Allen, J.F.: State transition – a question of balance. – Science **299**: 1530-1532, 2003.

Barber, J., Kühlbrandt, W.: Photosystem II. – Curr. Opin. Struct. Biol. **9**: 469-475, 1999.

Blankenship, R.E.: Molecular Mechanisms of Photosynthesis. – Blackwell Science, 2002.

Boekema, E.J., van Roon, H., van Breemen, J.F.L., Dekker, J. P.: Supramolecular organization of photosystem II and its light-harvesting antenna in partially solubilized photosystem II membranes. – Eur. J. Biochem., **266**: 444-452, 1999.

Boekema, E.J., van Breemen, J.F.L., van Roon, H., Dekker, J. P.: Conformational changes in photosystem II. Super-complexes upon removal of extrinsic subunits. – Biochemistry **39**: 12907-12915, 2000.

Croce, R., Müller, M.G., Bassi, R., Holzwarth, A.R.: Carotenoid-to-chlorophyll energy transfer in recombinant major light-harvesting complex (LHCII) of higher plants. I. Femtosecond transient absorption measurements. – Biophys. J. **80**: 901-915, 2001.

Dědic, F., Promnares, K., Pšenčík, J., Svoboda, A., Kořínek, M., Tichý, M., Komenda, J., Funk, C., Hála, J.: Hole burning study of cyanobacterial Photosystem II complexes differing in the content of small putative chlorophyll-binding proteins. – J. Lumin. **107**: 230-235, 2004.

Fetisova, Z.G., Mauring, K.: Investigation of structural organization of pigments in chlorosomal antenna of green bacteria *Chlorobium limicola* by spectral hole burning. – Biofizika **43**: 452-455, 1998.

Gibasiewicz, K., Szrajner, A., Ihalainen, J.A., Germano, M., Dekker J.P., van Grondelle, R.: Characterization of low-energy chlorophylls in the PSI-LHCI supercomplex from *Chlamydomonas reinhardtii*. A Site-Selective Fluorescence Study. – J. Phys. Chem. B **109**: 21180-21186, 2005.

Gillie, J.K., Lyle, P.A., Small, G.J., Golbeck, J.H.: Spectral hole burning of the primary electron donor state of Photosystem I. – Photosynth. Res. **22**: 233-246, 1989a.

Gillie, J.K., Small, G.J., Golbeck, J.H.: Nonphotochemical hole burning of the native antenna complex of photosystem I (PSI-200). – J. Phys. Chem. **93**: 1620-1627, 1989b.

Gobets, B., van Amerongen, H., Monshouwer, R., Kruip, J., Rögner, M., van Grondelle, R., Dekker, J.P.: Polarized site-selected fluorescence spectroscopy of isolated photosystem I particles. – Biochim. Biophys. Acta. **1188**: 75-85, 1994.

Groot, M.L., Dekker, J.P., van Grondelle, R., den Hartog, F.T.H., Volker, S.: Energy transfer and trapping in isolated photosystem II reaction centers of green plants at low temperature. A study by spectral hole burning. – J. Phys. Chem. **100**: 11488-11495, 1996.

Hála, J., Vácha, M., Dian, J., Prášil, O., Komenda, J.: Spectral hole burning of pea chloroplast chlorophyll-protein complexes in gel. – Photosynthetica **26**: 429-436, 1992.

Hayes, J.M., Matsuzaki, S., Rätsep, M., Small, G.J.: Red chlorophyll *a* antenna states of photosystem I of the cyanobacterium *Synechocystis* sp. PCC 6803. – J. Phys. Chem. B **104**: 5625-5633, 2000.

Ihalainen, J.A., Rätsep, M., Jensen, P.E., Scheller, H.V., Croce, R., Bassi, R., Korppi-Tommola, J.E.I., Freiberg, A.: Red spectral forms of chlorophylls in green plant PSI- a site-selective and high-pressure spectroscopy study. – J. Phys. Chem. B **107**: 9086-9093, 2003.

Jankowiak, R., Hayes, J.M., Small, G. J.: Spectral hole-burning spectroscopy in amorphous molecular solids and proteins. – Chem. Rev. **93**: 1471-1502, 1993.

Johnson, S.G., Lee, I.-J., Small, G. J.: Solid state line-narrowing spectroscopies. – In: Scheer, H. (ed.): Chlorophylls. Pp. 739-764, CRC Press, Boca Raton – Ann Arbor – Boston – London 1991.

Liu, Z.F, Yan, H.C., Wang, K.B., Kuang, T.Y., Zhang, J.P., Gui, L.L., An, X.M., Chang, W.R.: Crystal structure of spinach major lightharvesting complex at 2.72 angstrom resolution. – Nature **428**: 287-292, 2004.

Novoderezhkin, V. I., Palacios, M.A., van Amerongen, H., van Grondelle, R.: Excitation dynamics in the LHCII complex of higher plants: Modeling based on the 2.72 angstrom crystal structure. – J. Phys. Chem. B **109**: 10493-10504, 2005.

Peterman, E.J.G.: Chlorophylls and Carotenoids in Oxygenic Photosynthesis. – Ph.D. Thesis. Pp. 91-122. Vrije Universiteit, Amsterdam 1998.

Peterman, E.J.G., Pullerits, T., van Grondelle, R., van Amerongen, H.: Electron-phonon coupling and vibronic fine structure of light-harvesting complex II of green plants: Temperature dependent absorption and high-resolution fluorescence spectroscopy. – J. Phys. Chem. B **101**: 4448-4457, 1997.

Pieper, J., Rätsep, M., Jankowiak, R., Irrgang, K.-D., Voigt, J., Renger G., Small, G.J.: Qy-level structure and dynamics of solubilized light-harvesting complex II of green plants: Pressure and hole burning studies. – J. Phys. Chem. A **103**: 2412-2421, 1999.

Pieper, J., Schodel, R., Irrgang, K.-D. Voigt, J., Renger, G.: Electron-phonon coupling in solubilized LHC II complexes of green plants investigated by line-narrowing and temperature-dependent fluorescence spectroscopy. – J. Phys. Chem. B **105**: 7115-7124, 2001.

Rätsep, M., Johnson, T.W., Chitnis, P.R., Small, G.J.: The red-absorbing chlorophyll *a* antenna states of photosystem I: A hole-burning study of Synechocystis sp. PCC 6803 and its mutants. – J. Phys. Chem. B **104**: 836-847, 2000.

Rätsep, M., Hunter, C.N., Olsen, J.D., Freiberg, A.: Band structure and local dynamics of excitons in bacterial light-harvesting complexes revealed by spectrally selective spectroscopy. – Photosynth. Res. **86**: 37-48, 2005.

Rätsep, M., Freiberg, A.: Electron–phonon and vibronic couplings in the FMO bacteriochlorophyll a antenna complex studied by difference fluorescence line narrowing. – J. Lumin. **127**: 251-259, 2007.

Rätsep, M., Pieper, J., Irrgang, K.-D., Freiberg, A.: Excitation wavelength-dependent electron-phonon and electron-vibrational coupling in the CP29 antenna complex of green plants. – J. Phys. Chem. B **112**: 110-118, 2008.

Reddy, N.R.S., van Amerongen, H., Kwa, S.L.S., van Grondelle, R., Small, G.J.: Low-energy exciton level structure and dynamics in light harvesting complex II trimers from the Chl a/b antenna complex of photosystem II. – J. Phys. Chem. **98**: 4729-4735, 1994.

Reinot, T., Zazubovich, V., Hayes, J.M., Small, G.J.: New insights on persistent nonphotochemical hole burning and its application to photosynthetic complexes. – J. Phys. Chem. B **105**: 5083-5098, 2001.

Ruban, A.V., Young, A.J., Pascal, A.A., Horton, P.: The effects of lllumination on the xanthophyll composition of the

photosystem II light-harvesting complexes of spinach thylakoid membranes. – Plant Physiol. **104**: 227-234, 1994.

Ruban, A.V., Berera, R., Ilioaia, C., van Stokkum, I.H.M., Kennis, J.T.M., Pascal, A.A., van Amerongen, H., Robert, B., Horton, P., van Grondelle, R.: Identification of a mechanism of photoprotective energy dissipation in higher plants. – Nature **450**: 575-578, 2007.

Timpmann, K., Rätsep, M., Hunter, C. N., Freiberg, A.: Emitting excitonic polaron states in core LH1 and peripheral LH2 bacterial light-harvesting complexes. – J. Phys. Chem. B **108**: 10581-10588, 2004.

van Amerongen, H., van Grondelle, R.: Understanding the energy transfer function of LHCII, the major light-harvesting complex of green plants. – J. Phys. Chem. B **105**: 604-617, 2001.

van Grondelle, R., Novoderezhkin, V.I.: Energy transfer in photosynthesis: experimental insights and quantitative models. – Phys. Chem. Chem. Phys. **8**: 793-807, 2006.

Wolf, J., Law, K.-Y., Myers, A.B.: Hole-burning subtracted fluorescence line-narrowing spectroscopy of squaraines in polymer matrices. – J. Phys. Chem. **100**: 11870-11882, 1996.

Zazubovich, V., Matsuzaki, S., Johnson, T.W., Hayes, J.M., Chitnis, P.R., Small, G. J.: Red antenna states of photosystem I from cyanobacterium *Synechococcus elongatus*: a spectral hole burning study. – Chem. Phys. **275**: 47-59, 2002.